

Protein kinase A mediates inhibition of the thrombin-induced platelet shape change by nitric oxide

Baard Olav Jensen, Frode Selheim, Stein Ove Døskeland, Adrian R. L. Gear, and Holm Holmsen

The thrombin-induced platelet shape change was blocked by nitric oxide (NO), as revealed by scanning electron microscopy, light transmission, and resistive-particle volume determination. The inhibitory effect of NO was accompanied by an increase in levels of both cyclic guanosine monophosphate (cGMP) and cyclic adenosine monophosphate (cAMP) and phosphorylation of the vasodilator-stimulated phosphoprotein (VASP). However, the inhibition of the shape change was only mimicked by cAMP analogs (Sp-5,6-DCl-cBIMPS, 8-AHA-cAMP, and 8-CPT-cAMP) and not by cGMP analogs (8-Br-PET-cGMP, 8-Br-cGMP, and 8-pCPT-cGMP). The

effect of NO on the thrombin-induced shape change was prevented by the protein kinase A (PKA) antagonists Rp-8-Br-cAMPS and Rp-cAMPS. The protein kinase G (PKG) antagonist Rp-8-CPT-cGMPS strongly inhibited PKG-mediated 46-kDa VASP Ser239 phosphorylation, but did not inhibit the thrombin-induced shape change or the PKA-mediated VASP Ser157 phosphorylation. Whereas an inhibitor of cyclic nucleotide phosphodiesterase (PDE) 3A (milrinone) mimicked the effect of NO, inhibitors of PDE2 (erythro-9-(2-hydroxy-3-nonyl)adenine) and PDE5 (dipyridamole) were poorly effective. We concluded that (1) NO was a potent and

reversible inhibitor of the platelet shape change, (2) the shape change was reversible, (3) the inhibitory effect of NO was mediated through activation of PKA, (4) the onset of the NO effect coincided with VASP Ser157 phosphorylation, and (5) removal of NO and platelet shape change coincided with VASP Ser157 dephosphorylation. These findings are compatible with elevation of cGMP by NO in a compartment close to PDE3A, PKA, and VASP, leading to a local increase of cAMP able to block thrombin-induced shape change. (Blood. 2004;104:2775-2782)

© 2004 by The American Society of Hematology

Introduction

When platelets are stimulated, they rapidly change shape from discoids to spheres possessing extensive pseudopodia.¹⁻³ This shape change precedes aggregation, secretion, and activation of the coagulation cascade.^{1,2,4} In healthy individuals, 65% to 90% of circulating platelets are discoidal,² and increased numbers of spherical platelets have been associated with vascular diseases.⁵ Shape change could therefore be an important step in hemostasis and thrombosis. Activation of the platelet shape change by thrombin has been extensively studied *in vitro*, but little is known about mechanisms inhibiting this process. Thrombin, a potent platelet agonist that induces shape change, aggregation, and secretion through many signaling systems⁶ is formed *in vivo*, in significant amounts at the site of a vascular injury, stimulating both platelet activation and overall thrombus growth.⁷⁻¹²

Regulation of platelet activation is an important physiologic function of the vascular endothelium including release of nitric oxide (NO),¹³ a potent inhibitor of platelet aggregation, secretion, adhesion, and binding of fibrinogen to integrin glycoprotein IIb/IIIa (GpIIb/IIIa).¹⁴⁻¹⁷ Conflicting results have, however, been reported about the effect of NO on shape change.¹⁸⁻²¹ The inhibitory effects of NO on platelet activation have been considered to be due to activation of the soluble guanylyl cyclase causing production of cyclic guanosine monophosphate (cGMP) and subsequent activation of cGMP-dependent protein kinase G (PKG).²² However, elevation of cGMP levels could lead to an increase of cyclic

adenosine monophosphate (cAMP) levels causing activation of protein kinase A (PKA). The mechanisms are likely to be mediated through inhibition of the type III, cGMP-inhibited, phosphodiesterase enzyme 3A (PDE3A).²³⁻²⁵ Activation of PKA and PKG causes phosphorylation of a number of proteins that may mediate inhibitory effects. A major substrate for PKA and PKG is the vasodilator-stimulated phosphoprotein (VASP),²⁶ which is phosphorylated at 3 distinct residues, Ser157, Ser239, and Thr278. However, Ser239 and Ser157 are phosphorylated preferentially by PKA and PKG, respectively.²⁷ PKA-induced phosphorylation of Ser157, but not Ser239 or Thr278, leads to a mobility shift of the VASP protein in sodium dodecyl sulfate-polyacrylamide gel electrophoresis (SDS-PAGE) from 46 kDa to 50 kDa, which correlates with fibrinogen receptor inhibition.¹⁷ Phosphorylation of GP1b (24 kDa) and the thromboxane A₂ (TxA₂) receptor (48-53 kDa) may contribute to inhibition of platelet activation,²⁸ whereas the effects of phosphorylation of other peptides, such as rap1B, remains unknown.²⁹ The intracellular signaling effects caused by NO are not fully understood but involve inhibition of phospholipase C and inositol triphosphate (IP₃)-mediated mobilization of [Ca⁺⁺]_i.^{30,31}

The current study investigates the effect of NO on the thrombin-induced platelet shape change done *in vitro* by infusing solutions of NO into suspensions of aspirin-treated, gel-filtered human platelets in the presence of creatine phosphate/creatine phosphokinase (CP/CPK).^{32,33} The effects of NO on the shape change were

From the Sections of Biochemistry and Molecular Biology and Anatomy and Cell Biology, Department of Biomedicine, University of Bergen, Bergen, Norway; and the Department of Biochemistry and Molecular Genetics, University of Virginia Health Sciences Center, Charlottesville, VA.

Submitted March 30, 2004; accepted June 18, 2004. Prepublished online as *Blood* First Edition Paper, July 20, 2004; DOI 10.1182/blood-2004-03-1058.

Supported by the Research Council of Norway and the Blix Fund.

Reprints: Holm Holmsen, Section of Biochemistry and Molecular Biology, Department of Biomedicine, University of Bergen, Jonas Liesvei 91, N-5009 Bergen, Norway; e-mail: holm.holmsen@biomed.uib.no.

The publication costs of this article were defrayed in part by page charge payment. Therefore, and solely to indicate this fact, this article is hereby marked "advertisement" in accordance with 18 U.S.C. section 1734.

© 2004 by The American Society of Hematology

analyzed by several parameters including light transmission, resistive-volume measurements, scanning electron microscopy, and measurement of platelet F-actin. We also studied intracellular signaling mechanisms potentially responsible for the inhibitory effect of NO: changes in [cGMP] and [cAMP], and the state of VASP protein phosphorylation by both [³²P]-phosphorylation and immunoblotting of VASP Ser157 and Ser239. Our results suggest that the reversible inhibition of the shape change by NO was mediated by increased levels of cGMP, leading to elevation of cAMP (possibly through inhibition of PDE3A), and subsequent activation of PKA and phosphorylation of VASP Ser157.

Materials and methods

Materials

Adenosine, 8-Br-cGMP (8-bromo-cGMP), 8-pCPT-cAMP (8-[4-chlorophenylthio]-cAMP), and erythro-9-(2-hydroxy-3-nonyl)adenine (EHNA; Sigma, St Louis, MO) were dissolved in water. Milrinone (Sigma) and 8-pCPT-cGMP (8-(4-chlorophenylthio)-cGMP; Biolog, Bremen, Germany) were dissolved in dimethyl sulfoxide (DMSO). Dipyridamole (Sigma) was dissolved in ethanol. Rp-cAMPS ((Rp)-adenosine-3',5'-cyclic monophosphorothioate), Rp-8-Br-cAMPS (8-bromoadenosine-3',5'-cyclic monophosphorothioate, Rp-isomer), Rp-8-pCPT-cGMPS (8-[4-chlorophenylthio-guanosine]-3',5'-cyclic monophosphorothioate), 8-Br-PET-cGMP (β-phenyl-1), N²-etheno-8-bromoguanosine-3',5'-cyclic monophosphate, and Sp-5,6-DCL-cBIMPS (5,6-dichloro-1-β-D-ribofuranosylbenzimidazole-3',5'-cyclic monophosphorothioate, Sp-isomer), and 8-pCPT-2'-O-Me-cAMP, 8-AHA-cAMP (Biolog) were dissolved in water. Dimethylarsinic acid and glutaraldehyde were from Merck (Darmstadt, Germany). OsO₄ was from EML (Berkshire, United Kingdom). Bovine thrombin (Parke-Davis, Morris Plains, NJ), CP, and CPK (Sigma) were dissolved in 0.15 M NaCl. Bovine serum albumin (BSA), fraction V (pH 7, lyophilized), was from ICN Biomedicals (Aurora, OH). Cyclic nucleotide phosphodiesterase (P-0134, from bovine heart) was from Sigma. [³²P]orthophosphate (carrier-free, code PBS-11), [U-¹⁴C]adenine (10.1 MBq/mmol;), and [5',8'-³H]cAMP (1.96 GBq/mmol) were from Amersham (Buckinghamshire, United Kingdom). [8-¹⁴C]guanine hydrochloride (2.07 MBq/mmol), and [8-³H]cGMP (0.38 GBq/mmol) were from Dupont (Dreieich, Germany). Monoclonal antibody (mAb)-VASP-5C6 was from Nanotools Antikoerper-technik (Teningen, Germany). Anti-VASP, mAb VASP-16C2, and anti-rabbit IgG (horseradish peroxidase conjugated) were from Transduction Laboratories (Lexington, KY).

Platelet isolation

Blood was obtained from healthy volunteers who denied having taken any medication within 10 days and was placed into 0.15 volume of 85 mM trisodium citrate/71 mM citric acid/100 mM glucose (ACD). Platelet-rich plasma (PRP) was prepared by centrifuging the blood for 6 minutes at 535g at room temperature. The platelets in PRP were sedimented by centrifugation at 1200g for 10 minutes and the platelet pellet suspended in one-third volume of autologous plasma (concentrated PRP) that was incubated for 15 minutes at 37°C with acetylsalicylic acid (8 mM final concentration; NMD, Oslo, Norway). The platelets were then transferred into a Ca⁺⁺-free Tyrode solution (136 mM NaCl, 2.7 mM KCl, 0.77 mM NaH₂PO₄ × 2H₂O, and 2.0 mM MgCl₂ × 6H₂O, pH 7.3) containing 5 mM glucose and 0.05% BSA by gel filtration through Sepharose CL-2B. Platelet counts were adjusted with Tyrode solution to 3.5 × 10⁸ platelets/mL, and suspensions were incubated at 37°C for at least 30 minutes before beginning the experiments. To minimize platelet aggregation that would interfere with measurement of shape change, all experiments were performed at low doses of thrombin (0.05-0.15 U/mL) with aspirin-treated platelets in the presence of the ADP-scavenging system CP/CPK, as described previously.³²

Light transmission monitoring

This was done at 37°C in a Payton dual-channel aggregation module (Payton Associates, Buffalo, NY) using polypropylene vials and Teflon-

coated stirring bars (1000 rpm). Shape change is indicated as a decrease in light transmission through the suspension (in contrast to platelet aggregation, which causes an increase in light transmission) and as a decrease in the amplitude of signal oscillations, resulting from varying orientations of discoid platelets in the light beam, which vanishes when the platelets become spherical.³⁴ It should be noted that the shape change is presented graphically in this paper as a downward deflection in the traces.

Resistive-volume measurements

Aliquots were mixed with 5 volumes of dimethylarsinic acid/sucrose (112 mM/111 mM) buffer containing 2% glutaraldehyde, pH 7.2. Analyses were performed with a Channelyzer C-1000 (Coulter Electronics, Luton, United Kingdom) connected to a Model ZM resistive counter (Coulter Electronics) fitted with a 100-μm aperture. Calibration was performed with monosized (2-μm diameter) polymer particles (Dyno Particles, Oslo, Norway) and the resolution was 0.148 fl/channel. Platelets with volumes between 2.6 and 17.3 fL were counted. Single-platelet disappearance, reflecting platelet aggregation,³⁵ was assessed by counting 0.5 mL of a diluted sample.

Scanning electron microscopy

Initial sample preparation was the same as for the resistive-volume measurements, and subsequent procedures were as described by Gear³⁶; staining was with 1% OsO₄, dehydration was in graded ethanol concentrations, and critical-point drying using CO₂. The dried samples were sputter-coated with gold and palladium (Polaron SEM Coating System, Polaron Equipment, Watford, United Kingdom). Morphologic classification was determined on micrographs taken with a Jeol JSM-T200 scanning microscope (Jeol, Tokyo, Japan) at × 5400 magnification; micrographs for illustrations were taken using a Jeol JEM-100CX electron microscope (Jeol) at × 7000 magnification.

Platelet F-actin content

Measurements were performed by a rhodamine/phalloidin-based flow cytometric assay, where fluorescence of bound rhodamine-phalloidin is proportional to the F-actin content.³⁷ Aliquots were fixed with an equal volume of BSA-free Tyrode solution containing 4% paraformaldehyde for 30 minutes at room temperature prior to sedimentation at 7000g for 10 minutes. The platelet pellets were resuspended in twice their original volume in BSA-free Tyrode solution containing 2% paraformaldehyde. Platelets were permeabilized with 0.1% Triton X-100 and incubated with 13 μM rhodamine-phalloidin for 30 minutes at room temperature prior to analysis in a Becton Dickinson FACS Sort Flow Cytometer (Becton Dickinson, San Jose, CA). The samples were gated for platelets based on their forward and side scatter profile, and mean fluorescence was calculated. Results are expressed as percent F-actin (based on 40% F-actin in unstimulated platelets^{37,38}).

Cyclic nucleotide levels

A modified prelabeling technique²³ was used. Concentrated PRP was incubated with 18 μM [8-¹⁴C]guanine hydrochloride or 1.8 μM [U-¹⁴C]adenine for 1 hour at 37°C before gel filtration. Incubation of gel-filtered platelets (GFP) mixtures was terminated by addition of 9 volumes of 50% ice-cold trichloroacetic acid. A recovery marker, [8-³H]cGMP or [5',8'-³H]cAMP, was added to each sample. The samples were centrifuged at 7000g for 5 minutes, and cyclic nucleotides were isolated by ion exchange chromatography on Dowex AG 50W-X-4 columns (Bio-Rad Laboratories, Hercules, CA). Aliquots for isolation of cGMP were applied to columns equilibrated with 0.05 N HCl. The columns were washed with 9 mL 0.05 N HCl, and cGMP was eluted with an additional 10 mL 0.05N HCl and collected as 1-mL fractions. For isolation of cAMP, aliquots were applied to columns equilibrated with distilled water. Columns were washed with 20 mL distilled water, and cAMP was eluted with an additional 20 mL distilled water and collected as 1-mL fractions. The aliquots containing cAMP and cGMP were then acidified by addition of 100 μL 1 N HCl to increase solubility in the scintillation fluid (Opti-Fluor; Packard, Meriden, CT), which was added to the samples, and the [³H] and [¹⁴C] radioactivities were determined in a Beckman LS 6000 LL liquid scintillation system (Beckman

Instruments, Fullerton, CA). The counts were corrected for crossover, and the recovery of [^3H]cGMP (about 70%) or [^3H]cAMP (about 60%) determined. Levels of [^{14}C]cGMP and [^{14}C]cAMP were expressed as percentages of total [^{14}C] radioactivity incorporated into the platelets. The actual values of cAMP and cGMP are based on 2.6 μmol metabolic adenylates and 1.0 μmol metabolic guanylates/ 10^{11} platelets.³⁹⁻⁴³ The purity of isolated cyclic nucleotides was verified by a phosphodiesterase assay. Isolated fractions of cyclic nucleotides were pooled, trichloroacetic acid was removed by repetitive washings with water-saturated diethyl ether, freeze-dried, and resuspended in 25 mM Tris (tris(hydroxymethyl)amino-methane)-HCl (pH 7.5) containing 10 mM MgSO_4 . The samples were then split and incubated with cyclic nucleotide phosphodiesterase (1 U/mL) for 2 hours at 37°C. Incubations were terminated by addition of 9 volumes 50% ice-cold trichloroacetic acid and subsequent separation was performed as described. Cyclic nucleotide phosphodiesterase (1 U/mL) was added to coincubated controls only after the addition of 5% trichloroacetic acid. This phosphodiesterase treatment caused loss of 82% of the radioactivity in peaks isolated from [$8\text{-}^{14}\text{C}$]guanine-labeled platelets (stimulated with NO) and 97% of the radioactivity in [$U\text{-}^{14}\text{C}$]adenine-labeled platelets (stimulated with 10 μM adenosine and 10 μM milrinone).

Protein phosphorylation and Western blotting

Parallel to the platelet shape change analyses, samples were processed to study VASP phosphorylation. Platelets were incubated in the absence or presence of cyclic nucleotide analogs for 15 to 30 minutes before incubation with NO for 0.5 to 1 minute. Aliquots were lysed and immunoblotted with mAb-16C2, which recognizes VASP only when Ser239 is phosphorylated, or with mAb-5C6, which recognizes VASP only when Ser157 is phosphorylated. Aliquots were mixed with equal volumes of sample buffer (62.5 mM Tris-HCl, pH 6.8, 20% glycerol, 2% sodium dodecyl sulfate (SDS), 5% mercaptoethanol), cleared by centrifugation at 7000g for 5 minutes, sonicated for 5 minutes, and heated for an additional 5 minutes at 95°C. The proteins were separated on 5% to 15% linear gradient reducing SDS-polyacrylamide gels. Immunodetection was performed on platelet proteins electroblotted on to 0.2- μm Protran Nitro-cellulose membranes (BA 83; Schleicher & Schuell, Dassel, Germany), using a wet transfer system (25 mM Tris, 190 mM glycine, 20% MeOH), and the residual protein-binding capacity of the membrane was saturated with a TBS-Tween solution (20 mM Tris, 137 mM NaCl, 0.1% Tween) containing 5% nonfat milk for 1 hour at room temperature. Incubation with primary and secondary antibody was carried out for 1 hour each, with repetitive washings in between. The membrane blot was developed with enhanced chemiluminescence (ECL) and recorded on a LAS-1000 phosphorimaging device or on Fuji RX medical x-ray films. [^{32}P]Protein phosphorylation was determined using [^{32}P]orthophosphate-prelabeled (18.5-37 MBq/mL) platelets as described elsewhere.³²

NO solutions

Preparation of NO solutions and determination of their NO content is described elsewhere.³³ The NO-containing solution was infused into platelet suspensions at a steady rate by a motor-driven syringe pump (using gas-tight syringes) and the amount of NO infused is expressed as mole NO per milliliter platelet suspension per minute (mol NO/mL/min).

Statistics

Results are expressed as means with SEM. Resistive-particle volumes are given as geometric means (mean platelet volume [MPV]), and the significance of any difference was assessed by the paired Student *t* test on log MPV values. Platelet morphology was assessed as described previously³⁶; scanning electron microscope pictures taken from 10 randomly selected areas on the filter under observation were examined. This analysis of platelet morphology was done blind; that is, samples were scrambled before processing, and the code not broken until the analysis was complete. Platelet shapes were classified into discs, discs possessing pseudopodia, and spherical cells possessing pseudopodia; at least 200 platelets on each filter were counted. Results were finally expressed as percentages and tested by Shapiro-Francia *W'* test for nonnormality. Only 2 of the 21 ratios (Figure 3) showed signs of nonnormality ($0.01 < P < .10$), possibly from single

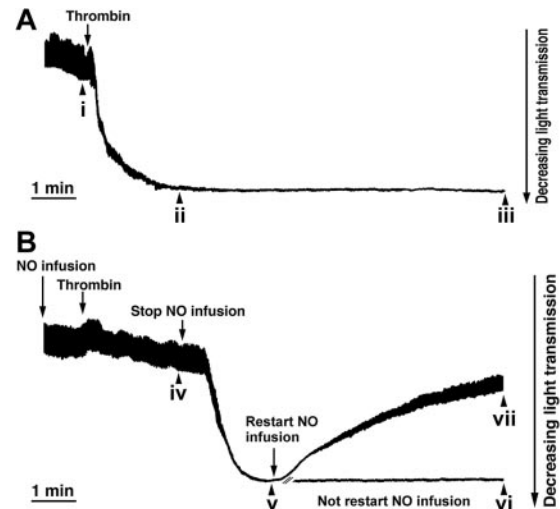


Figure 1. NO is a reversible inhibitor of the thrombin-induced shape change. Aspirin-treated and gel-filtered human platelets in the presence of CP/CPK were stimulated with thrombin (0.01 U/mL) and exposed to NO (1.1×10^{-10} mol NO/mL/min, as indicated), and platelet shape change is consistent with a decrease in light transmission (see "Materials and methods"). (A) Shape change induced by thrombin (0.01 U/mL). (B) NO infusion was started 1 minute prior to the addition of thrombin. Two minutes after the addition of thrombin, NO infusion was stopped, and 2 minutes later, infusion of NO was restarted. Aliquots were withdrawn (i-vii) for the analysis of platelet resistive-volume and platelet morphology (Figures 2 and 3). Traces are from a single experiment, representative of 6.

outliers. We therefore regarded the ratios as normally distributed, and the significance of any difference was assessed with the paired Student *t* test.

Results

To study the effects of NO on platelet shape change, we modified a light-transmission assay^{44,45} in which platelet aggregation (which would interfere with the determination of shape change) was minimized by using a low concentration of thrombin in combination with aspirin and CP/CPK (see "Materials and methods"). The extent of platelet aggregation during these experiments was always less than 5% compared to nonstimulated platelets, assessed by single-platelet disappearance (data not shown). This assay system was used routinely. Shape change was verified by resistive-volume measurements and by scanning electron microscopy.

Rapid, reversible inhibition of the thrombin-induced shape change by NO

NO totally inhibited the thrombin-induced shape change (Figures 1, 2, and 3). Moreover, the inhibitory effects of NO at 1.1 to 21.2×10^{-10} mol NO/mL/min were fully reversible, although there was a dose-dependent lag phase between stopping infusion of NO and recovery of the shape change with increasing NO concentration (results not shown). This effect was due to delayed auto-oxidation of NO at higher infusion rates and was rapidly reversed by scavenging NO by methemoglobin (results not shown). Thrombin stimulation caused a decrease in the number of discoid platelets (5% [B] versus 73% [A]; $P < .05$; $n = 4$) and produced an increase mainly in spherical cells possessing pseudopodia (94% [B] versus 5% [A], $P < .05$; $n = 4$; Figures 2 and 3). These responses were prevented by NO (Figures 2 and 3; treatment D), but readily reversed on stopping NO infusion, observed both as a decrease in discoid platelets (16% [E] versus 80% [D]; $P < .05$; $n = 4$) and also by an increase in spherical cells possessing pseudopodia (83% [E] versus 1% [D]; $P < .05$; $n = 4$; Figures 2 and 3).

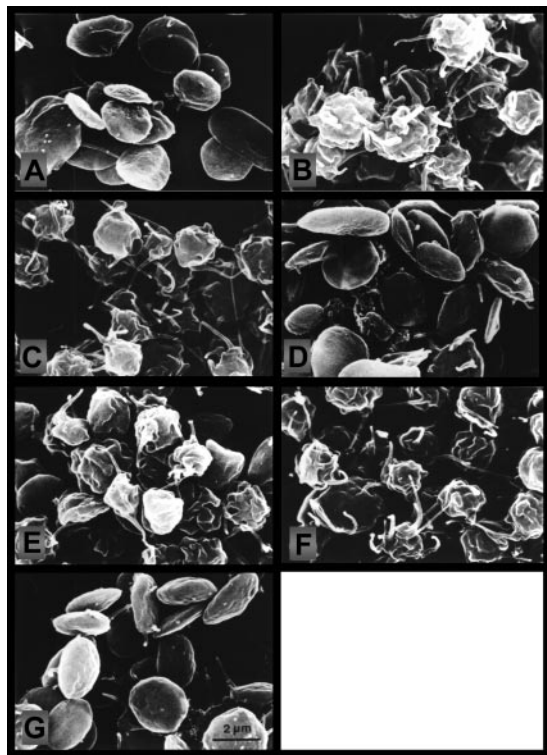


Figure 2. Effect of NO on the thrombin-induced changes in platelet morphology. Scanning electron micrographs prepared from aliquots withdrawn as depicted by letters i-vii in Figure 1 and Figure 3. (A) Control (stirred 1 minute); (B) thrombin (2 minutes); (C) thrombin (10 minutes); (D) NO (1 minute) followed by NO and thrombin together (2 minutes); (E) NO (1 minute) plus NO and thrombin together (2 minutes), then stop of NO infusion (2 minutes); (F) NO (1 minute) plus NO and thrombin together (2 minutes), then stop of NO infusion (7 minutes); (G) NO (1 minute) plus NO and thrombin together (2 minutes), then stop of NO (2 minutes); then NO reinfusion (5 minutes). Micrographs are from a single experiment, representative of 4. The micrographs were photographed on the electron microscope screen with a Leica M2 camera, exposure time $\frac{1}{6}$ seconds, aperture 4, and a focal distance of 50 mm; screen magnification was 7000 \times .

Reversal of the shape change process in thrombin-stimulated platelets by NO

Samples i through vii in Figure 1 correspond to micrographs A through G in Figure 2 and to treatments A through G in Figure 3, respectively. We found that platelet shape change was readily reversed by NO, as evidenced by measurements of light transmission (Figure 1B) and platelet resistive-volumes and by analysis of cell morphology (on aliquots withdrawn as depicted in Figure 1 letters A-G; Figures 2 and 3). Resumption of NO infusion after the thrombin-induced shape change caused a major decrease in spherical cells possessing pseudopodia (from 83% [E] to 3% [G]; $P < .05$; $n = 4$), combined with an increase in discs possessing pseudopodia (45% [G] versus 1% [E]; $P < .05$; $n = 4$) and pure discs (52% [G] versus 16% [E]; $P < .05$; $n = 4$; Figures 2 and 3).

Platelet shape change is associated with an increase in F-actin.⁴⁶ Because NO reversed the morphologic appearance of shape change, we wanted to see if this implied a reversal of the increase in F-actin. Under the conditions used, thrombin (0.01 U/mL for 5 minutes) caused an increase of platelet F-actin content from 40% to 53% ($P < .05$; $n = 4$). Infusion of NO (1.1×10^{-10} mol NO/mL/min) for 5 minutes completely reversed this increase (42% versus 40%; $P = .38$; $n = 4$), whereas the F-actin content in a sample continuously stimulated by thrombin (5 + 5 minutes) remained stable (54% versus 53%; $P = .89$; $n = 4$).

NO also inhibited shape change induced by direct activation of G-proteins

Agents that elevate cAMP levels in platelets have been described to reduce thrombin binding,⁴⁷ which therefore could be a mechanism involved in the inhibition of the thrombin-induced shape change by NO. Because AlF_4^- activates G-proteins directly,^{48,49} we tested the effects of NO on AlF_4^- -induced shape change monitored as shown in Figure 1. AlF_4^- (5.6 mM NaF and 1.9 μM AlCl_3) induced a shape change comparable to that of thrombin, which was blocked by NO (1.4×10^{-10} mol NO/mL/min) given 5 minutes after addition of AlF_4^- (data not shown).

NO increases both platelet cGMP and cAMP levels

Inhibition of thrombin-induced shape change by NO was associated with increased levels of both cGMP and cAMP (Figure 4A). NO (2.1×10^{-10} mol/min/mL), which totally inhibited thrombin-induced shape change, induced a small elevation in the level of cAMP (2.2 to 2.8 nmol/ 10^{11} platelets, $P = .07$; $n = 4$; Figure 4A).

This increase can be contrasted with the effects of milrinone, a specific inhibitor of PDE3,⁵⁰ and adenosine, an activator of adenylyl cyclase.⁵¹ Milrinone (10 μM) and adenosine (10 μM) increased the level of cAMP from 2.2 to 3.2 and 4.8 nmol/ 10^{11} platelets, respectively ($P < .05$; $n = 4$; Figure 4A). In addition, both NO and milrinone enhanced the adenosine-induced elevation of cAMP (Figure 4A).

Milrinone inhibited thrombin-induced shape change (Figure 4B) even at concentrations (1-5 μM) below that (10 μM) used to demonstrate cAMP elevation (Figure 4A). In contrast, inhibitors of PDE2 (EHNA; 10-100 μM) and PDE5 (dipyridamol; 1-10 μM) failed to inhibit thrombin-induced platelet shape change (data not shown). Therefore, inhibition of PDE3 by cGMP may well contribute to the modest elevation of cAMP level seen in the presence of NO.

Membrane-permeable cyclic nucleotide analogs demonstrate that NO-induced inhibition of thrombin-induced shape change is mediated by PKA, not PKG

Consistent with the hypothesis that cGMP and PKG activation mediate the inhibitory effects of NO, we examined the inhibitory effects of membrane-permeable cGMP analogs. However, only cAMP and not cGMP analogs inhibited thrombin-induced platelet shape change. 8-Br-PET-cGMP (0.5 mM), 8-Br-cGMP (1 mM), and 8-pCPT-cGMP (1 mM) all failed to inhibit the shape change induced by thrombin (0.01 U/mL), although all analogs strongly

Treatment	Time (min)	Morphology			
		MPV (fL)	Discs (%)	Discs with pseudopods (%)	Spherical cells with pseudopods (%)
(A) Control (start experiment)	0	7.1 \pm 0.3	73 \pm 5	21 \pm 5	5 \pm 2
(B) Thrombin	5	7.7 \pm 0.3*	5 \pm 2*	1 \pm 1*	94 \pm 2*
(C) Thrombin	10	7.6 \pm 0.3*	7 \pm 7*	1 \pm 1*	92 \pm 7*
(D) NO Thrombin	5	6.9 \pm 0.3	80 \pm 5	18 \pm 5	1 \pm 1*
(E) NO Thrombin	5	7.5 \pm 0.3*	16 \pm 3*	1 \pm 1*	83 \pm 4*
(F) NO Thrombin	5	7.6 \pm 0.3*	5 \pm 2*	0*	95 \pm 2*
(G) NO Thrombin	5	7.0 \pm 0.3*	52 \pm 12*	45 \pm 13*	3 \pm 1

Figure 3. Effects of NO on the thrombin-induced changes in platelet resistive-volume and platelet morphology. Aspirin-treated and gel-filtered human platelets in the presence of CP/CPK were stimulated with thrombin (0.01 U/mL; heavy blocks) and NO (1.1×10^{-10} mol NO/mL/min; narrow bars), as indicated by their respective boxes. Aliquots for resistive-volume measurement and assessment of platelet morphology were withdrawn at the end of each experiment (see "Materials and methods"). Control A indicates platelets at beginning of the experiments (30 minutes at 37°C after gel-filtration and then stirred for 1 minute). The treatments or sampling conditions are consistent with those indicated by letters i-vi in Figure 1. Results are mean values of 4 separate experiments \pm SEM. * $P < .05$ versus control A; † $P < .05$ versus treatments in E and F.

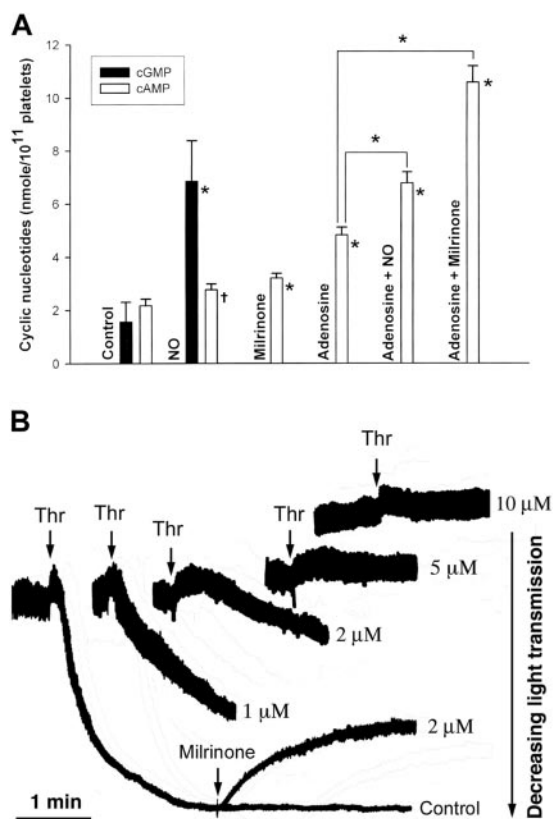


Figure 4. Levels of cAMP and cGMP in platelets treated with NO, adenosine, or milrinone. Effect of milrinone on the thrombin-induced shape change. (A) [¹⁴C]guanine-prelabeled or [¹⁴C]adenine-prelabeled, aspirin-treated, and gel-filtered human platelets in the presence of CP/CPK were exposed to NO (2.1×10^{-10} mol NO/mL/min) or adenosine ($10 \mu\text{M}$) for 1 minute, and to the phosphodiesterase inhibitor milrinone ($10 \mu\text{M}$) for 5 minutes. The agents were present alone or in combinations. Values are presented as means \pm SEM ($n = 3-11$). Determination of cyclic nucleotides is described in "Materials and methods." (B) The shape change induced by thrombin (0.01 U/mL) was studied as described in the legend to Figure 1, except that various concentrations ($0, 1, 2, 5,$ and $10 \mu\text{M}$) of milrinone were present for 5 minutes before the addition of thrombin or were added afterward as indicated. * $P < .05$ versus control (or as indicated), † $P = .07$ versus control.

inhibited (80%-100%) platelet aggregation induced by thrombin (0.06 U/mL ; data not shown). 8-Br-PET-cGMP is a potent agonist for PKG-I α and PKG-I β , whereas 8-pCPT-cGMP is a PKG-II agonist.⁵² An explanation why these analogs fail to mimic endogenous cGMP may be their poor ability to inhibit PDE3.^{49,53} In contrast, specific activators of PKA (Sp-5,6-DCI-cBIMPS [$50-200 \mu\text{M}$], 8-AHA-cAMP [$200 \mu\text{M}$], and 8-pCPT-cAMP [$500 \mu\text{M}$])⁵² inhibited both the shape change induced by thrombin (0.01 U/mL ; 64%-100% inhibition) and the platelet aggregation induced by thrombin (0.06 U/mL ; 69%-72% inhibition).

Next, we examined the effects of PKG and PKA antagonists. Only PKA antagonists, but not PKG antagonists, counteracted the inhibitory effect of NO. Rp-8-pCPT-cGMPS did not block NO-mediated inhibition of thrombin-induced shape change (Figure 5B), whereas inhibition of the shape change by NO was abolished in the presence of the PKA-antagonists Rp-8-Br-cAMPS and Rp-cAMPS (Figure 5C). Finally, to exclude the possibility that EPAC, cAMP-regulated guanine nucleotide exchange factor, played a role in the NO-mediated inhibition of shape change, we preincubated platelets with the specific EPAC activator 8-pCPT-2'-O-Me-cAMP⁵⁴ and found no effect on the shape change. Altogether, these data indicate a central role of PKA in mediating the NO-induced inhibition of the thrombin-induced shape change.

Phosphorylation of VASP Ser157 and not Ser239 correlated closely with the inhibitory effect of NO on thrombin-induced shape change

In a search for a potential mediator of PKA action on the platelet shape change, we studied the phosphorylation of VASP, which has been implicated in NO actions.²² Shape change was continuously monitored while aliquots were withdrawn (as indicated by nos. 1-12 in Figure 6A) for analysis of platelet VASP Ser157 phosphorylation and overall [³²P] incorporation into VASP (Figure 6B-C). We observed that NO-induced phosphorylation of VASP Ser157 shifted the apparent molecular mass of VASP from 46 to 50 kDa (Figure 6B-C). Moreover, the phosphorylation/dephosphorylation of VASP Ser157 closely followed the reversible inhibitory effects of NO on the thrombin-induced shape change (Figure 6A-C). The phosphorylation of pleckstrin (45 kDa) and a myosin light chain (20 kDa) coincided with the thrombin-induced shape change and was also reversibly inhibited by NO (Figure 6C). NO rapidly induced phosphorylation of both VASP Ser239 (PKG-mediated)

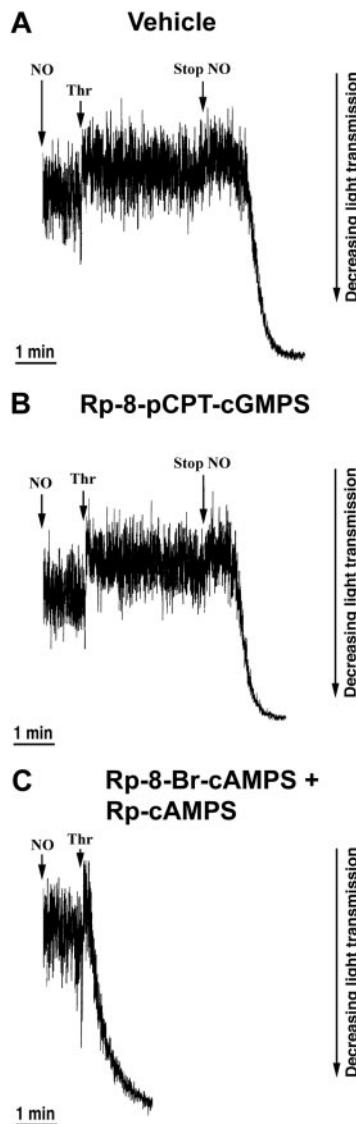


Figure 5. Effects of PKG and PKA inhibitors on the NO-mediated inhibition of the thrombin-induced shape change. Aspirin-treated and gel-filtered human platelets in the presence of CP/CPK were stimulated with thrombin (0.01 U/mL) and NO (1.1×10^{-10} mol NO/mL/min) after 30 minutes of preincubation with vehicle (water; A), 0.5 mM Rp-8-pCPT-cGMPS (B), or 0.5 mM Rp-8-Br-cAMPS plus 0.5 mM Rp-cAMPS (C). Traces are from a single experiment, representative of 3. The experimental conditions are as explained in the legend to Figure 1.

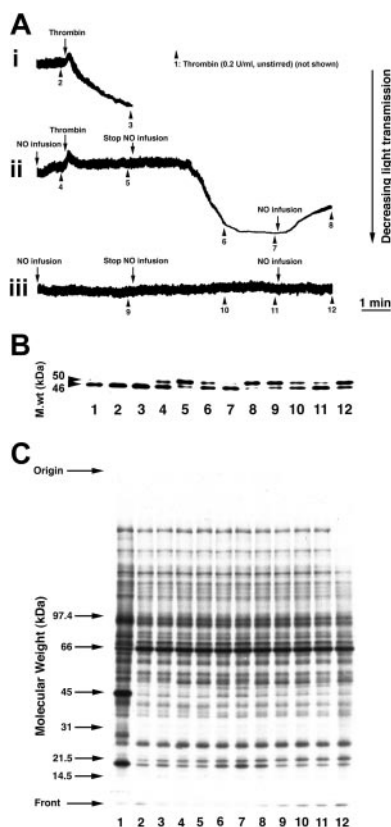


Figure 6. Correlation of the effects of NO on the thrombin-induced shape change and protein phosphorylation. [32 P]-prelabeled, aspirin-treated, and gel-filtered human platelets in the presence of CP/CPK were stimulated with thrombin (0.015 U/mL) and NO (1.7×10^{-10} mol NO/mL/min). Shape change was continuously monitored by light transmission (A traces i-iii). Aliquots were withdrawn (arrows 1-12) for determination of VASP Ser157 phosphorylation (B) and [32 P]-protein phosphorylation (C). (A) Trace i shows the effect of thrombin (without NO infusion); trace ii is the effect of intermittent NO infusion to the platelet suspension combined with addition of thrombin; and trace iii is the effect of intermittent NO infusion to the platelet suspension (without thrombin stimulation). (B) Western immunoblot of proteins separated by 5% to 15% linear gradient SDS-PAGE, probed with mouse anti-VASP. The numbers indicate the following: (1) thrombin (0.2 U/mL) for 5 minutes without stirring; (2) control (stirred for 1 minute); (3) thrombin from 1 to 3 minutes; (4) NO infusion from 0 to 1 minute; (5) NO infusion from 0 to 3 minutes, and thrombin stimulation from 1 to 3 minutes; (6) NO infusion from 0 to 3 minutes, and thrombin stimulation from 1 to 6 minutes; (7) NO infusion from 0 to 3 minutes, and thrombin stimulation from 1 to 8 minutes; (8) NO infusion from 0 to 3 minutes, and thrombin stimulation from 1 to 10 minutes, and NO infusion from 8 to 10 minutes; (9) NO infusion from 0 to 3 minutes; (10) NO infusion from 0 to 3 minutes, stop NO infusion from 3 to 8 minutes; (11) NO infusion from 0 to 3 minutes, stop NO infusion from 3 to 8 minutes; (12) NO infusion from 0 to 3 minutes, stop NO infusion from 3 to 8 minutes, and NO infusion from 8 to 10 minutes. (C) Aliquots from the same samples as in panel B were separated by 5% to 15% linear gradient SDS-PAGE and [32 P]-protein phosphorylation were visualized by autoradiography. The results shown are from a single experiment representative of 3.

and Ser157 (PKA-mediated; Figure 7). The PKG-antagonist Rp-8-CPT-cGMPs did not inhibit PKA-mediated VASP Ser157 phosphorylation, or shape change, but strongly inhibited PKG-mediated 46 kDa VASP Ser239 phosphorylation.

Discussion

Shape change is the first step in platelet activation, but the mechanisms of its physiologic regulation are poorly understood. Circulating platelets are exposed to endothelium-derived NO and low levels of thrombin,^{5,13,44,55-61} and alterations in NO concentrations might influence this balance, as evidenced by increased susceptibility to thrombosis in patients with impaired NO produc-

tion.⁶² We show here that NO prevents and reverses the thrombin-induced platelet shape change via a pathway dependent on PKA activation. The NO effect was rapidly reversible and occurred at concentrations produced by stimulated endothelial cells.^{63,64} Circulating platelets should thus be able to respond to fluctuations in plasma concentration of NO with a rapid and reversible shape change.

We found that NO caused spherical platelets possessing pseudopodia and ruffles to become normal discs, through intermediate stages of discs with pseudopodia (Figures 2 and 3). Shape change involves rapid actin filament assembly⁴⁶ and we demonstrated that thrombin-induced actin filament assembly was entirely reversed by NO. In our hands shape change occurred with only a modest increase in F-actin, that is, from 40% to 53% of total actin, whereas maximally activated platelets contain up to 70% F-actin. Apparently, actin polymerization occurs in 2 phases in thrombin-stimulated platelets: a rapid polymerization of modest magnitude associated with the shape change and a more extensive polymerization associated with aggregation.⁶⁵

NO stimulates guanylyl cyclase and, because cGMP is an established downstream effector of NO, we expected cGMP to be responsible for the action of NO. The major route of cGMP action is through activation of cGMP-dependent protein kinase (PKG). Furthermore, cGMP can enhance the accumulation of cAMP through inhibition of PDE^{323,50,66} (Figure 4). However, selective PKG antagonists failed to block NO-mediated effects on the shape change suggesting that PKG was not responsible for the NO-induced antagonism of the shape change. The PKG specificity of the antagonist Rp-8pCPT-cAMPS was demonstrated by its ability to selectively counteract phosphorylation of VASP at Ser239, which is preferentially phosphorylated by PKG,²⁷ in the NO-stimulated platelets.

Furthermore, selective stimulators of PKG did not inhibit the shape change. They penetrated the platelets as evidenced by their ability to counteract thrombin-induced platelet aggregation. These PKG agonists, like 8-pCPT-cGMP, are known to be quite stable toward hydrolysis by PDEs and neither affect the cGMP-activated

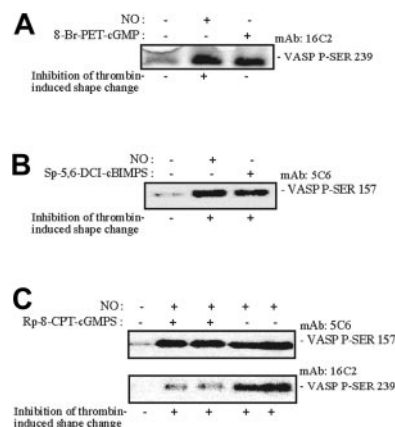


Figure 7. Effects of NO and selected cyclic nucleotide analogues on VASP Ser157 and VASP Ser239 phosphorylation. Aspirin-treated and gel-filtered human platelets were preincubated for 15 minutes in the absence or presence of a PKG activator (0.1 mM 8-Br-PET-cGMP) or PKA activator (0.2 mM SP-5,6-DCL-cBIMPS) or for 30 minutes with the PKG antagonist (0.5 mM Rp-8-pCPT-cGMPs). The platelets were then stimulated with thrombin (0.01 U/mL) alone or with NO (1.7×10^{-10} mol NO/mL/min) for 0.5 (A-B) or 1 minute (C) in the presence of CP/CPK. Shape change was monitored by light transmission, and aliquots were withdrawn for measurement of VASP phosphorylation using monoclonal anti-P-Ser157-VASP5C6 and anti-P-Ser239 antibodies as described in "Materials and methods." The 5C6 antibody recognizes phosphorylated VASP-Ser157 preferentially phosphorylated by PKA, whereas the VASP-16C2 antibody recognizes phosphorylated VASP Ser239 preferentially phosphorylated by PKG. The results are from a single experiment representative of 3.

nor the cGMP-stimulated PDEs in platelets.⁵³ In line with their selectivity as PKG agonists, they caused specific phosphorylation of VASP Ser239 (Figure 7).

We considered next whether the modest increase of cAMP in NO-exposed platelets could be responsible for inhibition of the shape change. We found that (1) VASP was phosphorylated at Ser157, which is preferentially targeted by PKA in NO-exposed cells, suggesting activation of PKA; (2) the effect of NO on shape change was blocked by cAMP phosphorothioate analogs specifically antagonizing PKA⁶⁷; and (3) selective activators of PKA mimicked the inhibitory effect of NO on shape change. We conclude, therefore, that PKA mediated the inhibition of shape change by NO.

We also considered whether cAMP could act via activation of the cAMP receptor EPAC, which is specifically activated by the cAMP analog 8-pCPT-2'-O-methyl-cAMP,^{54,68} and induces PKA-dependent neurite outgrowths.⁶⁸ This analog had no effect on the shape change, indicating that PKA was solely responsible for mediating the NO-induced inhibitory effect on shape change.

Phosphorylation of VASP at Ser157 correlated closely with the effect of NO on the shape change, both when NO was added and removed (Figure 6A-C), suggesting that phosphorylation of VASP-Ser157 is important in reversible inhibition of shape change. VASP is believed to help regulate actin filament assembly.⁶⁹ Our results show that VASP-Ser157 phosphorylation occurred with the right timing to interfere with VASP-mediated assembly of actin filaments during the shape change. It was recently reported that PKA-catalyzed VASP-Ser239 phosphorylation correlated temporally with inhibition of aggregation induced by elevation of cGMP in human platelets, and that PKG could activate rather than inhibit platelet aggregation.^{70,71} The authors did not study platelet shape change. Both Gambaryan et al⁷² and we ourselves (Figure 7, and S.O.D., unpublished observations, October 2003) failed to reproduce fully these findings. We conclude that whereas PKA is solely responsible for mediating inhibition of shape change by NO, both PKG and PKA may be responsible for mediating NO-induced inhibition of platelet aggregation. Based on our present studies on NO-mediated inhibition of thrombin-induced shape change, we suggest that the relevant signaling impact of elevated cGMP is to increase cAMP concentration possibly by inhibiting the cGMP-

inhibitable PDE3A.²³ In VASP-deficient mice, cAMP- and cGMP-mediated inhibition of platelet aggregation is strongly reduced,^{73,74} whereas platelet adhesion is enhanced and unresponsive to NO.⁷⁵ However, mechanisms other than activation of PKA and Ser157 phosphorylation of VASP may contribute to the inhibitory effects of NO on the shape change. Elevated concentrations of cAMP in platelets have been reported to influence a number of cell-signaling molecules or events,^{16,31,47,76-79} elevated levels of phosphatidylinositol 4-phosphate, reduced production of phosphatidylinositol 4,5-bisphosphate, inhibition of polyphosphoinositide-specific phospholipase C, reduced Ins-1,4,5-IP₃ formation, reduced Ca⁺⁺ mobilization and reduced binding of thrombin. The latter mechanism seems less likely to be responsible because we observed similar inhibitory effects of NO on AIF₄⁻-induced shape change, which bypasses receptor activation.^{48,49} The magnitude of the NO effect on VASP-Ser157 phosphorylation was surprising in view of the modest increase of cAMP and is compatible with a colocalization of PDE3, PKA, and VASP. This notion is supported by our observation that inhibitors of PDE2 and PDE5 were far less efficient than PDE3 inhibitor to block shape change, and by the observation by Manns et al⁸⁰ that a PDE3 inhibitor causes stronger phosphorylation of VASP than a PDE2 inhibitor, even if the latter induces a higher platelet cAMP level.

We conclude that the platelet shape change can be antagonized by PKA activation, which may occur with particular efficiency through the formation of a local compartment of cAMP through inhibition of PDE3. Whereas PKG has no apparent role in the platelet shape change, it can antagonize platelet aggregation. PKA agonists are therefore inhibitors of both the platelet shape change and aggregation, whereas PKG agonists only inhibit platelet aggregation.

Acknowledgments

We wish to thank the late Jakob Røli for assistance with the scanning electron microscopic procedures and Daniel Cejka for developing a computerized data acquisition system for the Coulter Channelyzer C-1000. Freshly drawn blood was provided by the Blood Bank at Haukeland Hospital, Bergen.

References

1. Wurzingler LJ. Histophysiology of the circulating platelet. *Adv Anat Embryol Cell Biol.* 1990;120:1-96.
2. Frojmovic MM, Milton JG. Human platelet size, shape, and related functions in health and disease. *Physiol Rev.* 1982;62:185-261.
3. Gear ARL, Polanowska-Grabowska R. The platelet shape change. In: Greslele P, Page CP, Fuster V, Vermynen J, eds. *Platelets in Thrombotic and Non-thrombotic Disorders: Pathophysiology, Pharmacology and Therapeutics.* Cambridge, United Kingdom: Cambridge University Press; 2002:319-337.
4. Zwaal RFA, Schroit AJ. Pathophysiologic implications of membrane phospholipid asymmetry in blood cells. *Blood.* 1997;89:1121-1132.
5. Milton JG, Frojmovic MM. Unusual properties of platelet shape in coronary and cerebral artery disease. *Thromb Res.* 1987;47:511-531.
6. Kanthou C, Benzakour O. Cellular effects of thrombin and their signalling pathways. *Cell Pharmacol.* 1995;2:293-298.
7. Weiss HJ. Flow-related platelet deposition on subendothelium [abstract]. *Thromb Haemost.* 1995;74:117.
8. Ginsberg MH, Xiaoping D, O'Toole TE, Loftus JC, Plow EF. Platelet integrins. *Thromb Haemost.* 1993;70:87-93.
9. Harker LA, Hanson SR, Kelly AB. Antithrombotic benefits and hemorrhagic risks of direct thrombin antagonists. *Thromb Haemost.* 1995;74:464-472.
10. Eidt JF, Allison P, Noble S, et al. Thrombin is an important mediator of platelet aggregation in stenosed canine coronary arteries with endothelial injury. *J Clin Invest.* 1989;84:18-27.
11. Pawashe AB, Golino P, Ambrosio G, et al. A monoclonal antibody against rabbit tissue factor inhibits thrombus formation in stenotic injured rabbit carotid arteries. *Circ Res.* 1994;74:56-63.
12. Badimon L, Badimon JJ, Lassila R, Heras M, Chesebro JH, Fuster V. Thrombin regulation of platelet interaction with damaged vessel wall and isolated collagen type I at arterial flow conditions in a porcine model: effects of hirudins, heparin, and calcium chelation. *Blood.* 1991;78:423-434.
13. Shimokawa H, Takeshita A. Endothelium-dependent regulation of the cardiovascular system. *Intern Med.* 1995;34:939-946.
14. Moncada S, Palmer RM, Higgs EA. Nitric oxide: physiology, pathophysiology, and pharmacology. *Pharmacol Rev.* 1991;43:109-142.
15. Welch GN, Upchurch GR, Loscalzo J. Nitric oxide as a vascular modulator. *Blood Rev.* 1995;9:262-269.
16. Blockmans D, Deckmyn H, Vermynen J. Platelet activation. *Blood Rev.* 1995;9:143-156.
17. Horstrup K, Jablonka B, Honig-Liedl P, Just M, Kochsiek K, Walter U. Phosphorylation of focal adhesion vasodilator-stimulated phosphoprotein at Ser157 in intact human platelets correlates with fibrinogen receptor inhibition. *Eur J Biochem.* 1994;225:21-27.
18. Broekman MJ, Eiroa AM, Marcus AJ. Inhibition of human platelet reactivity by endothelium-derived relaxing factor from human umbilical vein endothelial cells in suspension: blockade of aggregation and secretion by an aspirin-insensitive mechanism. *Blood.* 1991;78:1033-1040.
19. Morgan RO, Newby AC. Nitroprusside differentially inhibits ADP-stimulated calcium influx and mobilization in human platelets. *Biochem J.* 1989;258:447-454.
20. Buechler WA, Ivanova K, Wolfram G, Drummer C, Heim JM, Gerzer R. Soluble guanylyl cyclase and platelet function. *Ann N Y Acad Sci.* 1994;714:151-157.
21. Ivanova K, Schaefer M, Drummer C, Gerzer R. Effects of nitric oxide-containing compounds on

- increases in cytosolic ionized Ca²⁺ and on aggregation of human platelets. *Eur J Pharmacol*. 1993;244:37-47.
22. Schwarz UR, Walter U, Eigenthaler M. Taming platelets with cyclic nucleotides. *Biochem Pharmacol*. 2001;62:1153-1161.
 23. Maurice DH, Haslam RJ. Molecular basis of the synergistic inhibition of platelet function by nitrovasodilators and activators of adenylate cyclase: inhibition of cyclic AMP breakdown by cyclic GMP. *Mol Pharmacol*. 1990;37:671-681.
 24. Schmidt HHW, Lohmann SM, Walter U. The nitric oxide and cGMP signal transduction system: regulation and mechanism of action. *Biochim Biophys Acta*. 1993;1178:153-175.
 25. Beavo J. Cyclic nucleotide phosphodiesterases: Functional implications of multiple isoforms. *Physiol Rev*. 1995;75:725-748.
 26. Butt E, Abel K, Krieger M, et al. cAMP- and cGMP-dependent protein kinase phosphorylation sites of the focal adhesion vasodilator-stimulated phosphoprotein (VASP) in vitro and in intact human platelets. *J Biol Chem*. 1994;269:14509-14517.
 27. Smolenski A, Bachmann C, Reinhard K, et al. Analysis and regulation of vasodilator-stimulated phosphoprotein serine 239 phosphorylation in vitro and in intact cells using a phosphospecific monoclonal antibody. *J Biol Chem*. 1998; 273: 20029-20035.
 28. Wang G, Zhu Y, Halushka P, Lincoln T, Mendelsohn M. Mechanism of platelet inhibition by nitric oxide: in vivo phosphorylation of thromboxane receptor by cyclic GMP-dependent protein kinase. *Proc Natl Acad Sci U S A*. 1998;95:4888-4893.
 29. Grunberg B, Kruse HJ, Negrescu EV, Siess W. Platelet rap1B phosphorylation is a sensitive marker for the action of cyclic AMP- and cyclic GMP-increasing platelet inhibitors and vasodilators. *J Cardiovasc Pharmacol*. 1995;25:545-551.
 30. Nakashima S, Tohmatsu T, Hattori H, Okano Y, Nozawa Y. Inhibitory action of cyclic GMP on secretion, polyphosphoinositide hydrolysis and calcium mobilization in thrombin-stimulated human platelets. *Biochem Biophys Res Commun*. 1986; 135:1099-1104.
 31. Haynes DH. Effects of cyclic nucleotides and protein kinases on platelet calcium homeostasis and mobilization. *Platelets*. 1993;4:231-242.
 32. Jensen BO, Holmsen H. Nitric oxide (NO)-platelet interactions: inhibition is independent of the prostanoid and ADP pathways. *Platelets*. 1995;5:83-90.
 33. Jensen BO, Skeidsvoll J, Holmsen H. A polarographic method for measuring dissolved nitric oxide. *J Biochem Biophys Methods*. 1997;35:185-195.
 34. White JG. Combined nephelometric and electron microscopic study of platelet release reaction. *Thromb Diath Haemorrh*. 1970;42:73-78.
 35. Gear ARL. Rapid reactions of platelets studied by a quenched-flow approach: aggregation kinetics. *J Lab Clin Med*. 1982;100:866-886.
 36. Gear ARL. Rapid platelet morphological changes visualized by scanning-electron microscopy: kinetics derived from a quenched-flow approach. *Br J Haematol*. 1984;56:387-398.
 37. Hartwig JH, Bokoch GM, Carpenter CL, et al. Thrombin receptor ligation and activated Rac uncaps actin filament barbed ends through phosphoinositide synthesis in permeabilized human platelets. *Cell*. 1995;82:643-653.
 38. Fox JE. The platelet cytoskeleton. *Thromb Haemost*. 1993;70:884-893.
 39. Verhoeven AJM, Tysnes OB, Aarbakke GM, Cook CA, Holmsen H. Turnover of the phosphomonoester groups of polyphosphoinositol lipids in unstimulated human platelets. *Eur J Biochem*. 1987; 166:3-9.
 40. Lages B, Holmsen H, Weiss HJ, Dangelmaier C. Thrombin and ionophore A23187-induced dense granule secretion in storage pool deficient platelets: evidence for impaired nucleotide storage as the primary dense granule defect. *Blood*. 1983; 61:154-162.
 41. Hanington E, Jones RJ, Amess JAL. Platelet nucleotides in migraine [letter]. *Lancet*. 1982;829:437.
 42. D'Souza L, Glueck HI. Measurement of nucleotide pools in platelets using high pressure liquid chromatography. *Thromb Haemost*. 1977;38:990-1001.
 43. Ugurbil K, Holmsen H. Nucleotide compartmentation: radioisotopic and nuclear magnetic resonance studies. In: Gordon JL, ed. *Platelets in Biology and Pathology*. Vol 2. Amsterdam, The Netherlands: Elsevier/North-Holland; 1981:147-177.
 44. Born GV. Observations on the change in shape of blood platelets brought about by adenosine diphosphate. *J Physiol*. 1970;209:487-511.
 45. Michal F, Born GV. Effect of the rapid shape change of platelets on the transmission and scattering of light through plasma. *Nat New Biol*. 1971;231:220-222.
 46. Hartwig JH. Mechanisms of actin rearrangement mediating platelet activation. *J Cell Biol*. 1992; 118:1441-1442.
 47. Lerea KM, Glomset JA, Krebs EG. Agents that elevate cAMP levels in platelets decrease thrombin binding. *J Biol Chem*. 1987;262:282-288.
 48. Murer EH. G-proteins and platelet activation by fluoride. *Prog Clin Biol Res*. 1988;283:493-498.
 49. Deana R, Ruzzene M, Doni MG, Zoccarato F, Alexandre A. Cyclic GMP and nitroprusside inhibit the activation of human platelets by fluoroaluminate. *Biochim Biophys Acta*. 1989;1014:203-206.
 50. Sheth S, Colman R. Platelet cAMP and cGMP phosphodiesterases. *Platelets*. 1995;6:61-70.
 51. Haslam RJ, Davidson MML, Desjardins JV. Inhibition of adenylate cyclase by adenosine analogues in preparations of broken and intact human platelets. *Biochem J*. 1978;176:83-95.
 52. Schwede F, Maronde E, Genieser H, Jastorff B. Cyclic nucleotide analogs as biochemical tools and prospective drugs. *J Exp Pharmacol Therapeut*. 2000;87:199-226.
 53. Butt E, Nolte C, Schulz S, et al. Analysis of the functional role of cGMP-dependent protein kinase in intact human platelets using a specific activator 8-para-chlorophenylthio-cGMP. *Biochem Pharmacol*. 1992;43:2591-2600.
 54. Enserink JM, Christensen AE, de Rooij J, et al. A novel Epac-specific cAMP analogue demonstrates independent regulation of Rap1 and ERK. *Nat Cell Biol*. 2002;4:901-906.
 55. Pohl U, Busse R. EDRF increases cyclic GMP in platelets during passage through the coronary vascular bed. *Circ Res*. 1989;65:1798-1803.
 56. Pohl U, Nolte C, Bunse A, Eigenthaler M, Walter U. Endothelium-dependent phosphorylation of vasodilator-stimulated protein in platelets during coronary passage. *Am J Physiol*. 1994;266:H606-H612.
 57. Gear ARL. Preaggregation reactions of platelets. *Blood*. 1981;58:477-490.
 58. Ehrman M, Toth E, Fröjmovic MM. A platelet procoagulant activity associated with platelet shape change. *J Lab Clin Med*. 1978;92:393-401.
 59. Lu H, Menashi S, Garcia I, et al. C: reversibility of thrombin-induced decrease in platelet glycoprotein Ib function. *Br J Haematol*. 1993;815:116-123.
 60. Ruf A, Patscheke H. Flow cytometric detection of activated platelets: comparison of determining shape change, fibrinogen binding, and P-selectin expression. *Semin Thromb Haemost*. 1995;21: 146-157.
 61. Pribluda V, Rotman A. Dynamics of membrane-cytoskeleton interactions in activated blood platelets. *Biochemistry*. 1982;21:2825-2832.
 62. Freedman JE, Loscalzo J, Benoit SE, Valeri CR, Barnard MR, Michelson AD. Decreased platelet inhibition by nitric oxide in two brothers with a history of arterial thrombosis. *J Clin Invest*. 1996;97: 979-987.
 63. Tsukahara H, Gordienko DV, Goligorsky MS. Continuous monitoring of nitric oxide release from human umbilical vein endothelial cells. *Biochem Biophys Res Commun*. 1993;93:722-729.
 64. Kanai AJ, Strauss HC, Truskey GA, Crews AL, Grunfeld S, Malinski T. Shear stress induces ATP-independent transient nitric oxide release from vascular endothelial cells, measured directly with a porphyrinic microsensor. *Circ Res*. 1995;77: 284-293.
 65. Glenn JR, Spangenberg P, Heptinstall S. Actin polymerization and depolymerization in relation to platelet shape change, aggregation and disaggregation. *Platelets*. 1996;7:23-27.
 66. Fisch A, Michael-Hepp J, Meyer J, Darius H. Synergistic interaction of adenylate cyclase activators and nitric oxide donor SIN-1 on platelet cyclic AMP. *Eur J Pharmacol*. 1995;289:455-461.
 67. Gjertsen BT, Mellgren G, Otten A, et al. Novel(Rp)-cAMPS analogs as tools for inhibition of cAMP-kinase in cell culture. Basal cAMP-kinase activity modulates interleukin-1 beta action. *J Biol Chem*. 1995;270:20599-20607.
 68. Christensen AE, Selheim F, de Rooij J, et al. cAMP analog mapping of Epac1 and cAMP kinase. Discriminating analogs demonstrate that Epac and cAMP kinase act synergistically to promote PC-12 cell neurite extension. *J Biol Chem*. 2003; 278:35394-35402.
 69. Holt MR, Critchley DR, Brindle NPJ. Molecules in focus: The focal adhesion phosphoprotein, VASP. *Int J Biochem Cell Biol*. 1998;30:307-311.
 70. Li Z, Adijc J, Eigenthaler M, Du X. A predominant role for cAMP-dependent protein kinase in the cGMP-induced phosphorylation of vasodilator-stimulated phosphoprotein and platelet inhibition in humans. *Blood*. 2003;101:4423-4429.
 71. Li Z, Gu M, Feil R, et al. A stimulatory role for cGMP-dependent protein kinase in platelet activation. *Cell*. 2003;112:77-87.
 72. Gambaryan S, Geiger J, Schwarz UR, et al. Potent inhibition of human platelets by cGMP analogs independent of cGMP-dependent protein kinase. *Blood*. 2003;103:2593-2600.
 73. Hauser W, Knobloch KP, Eigenthaler M, et al. Megakaryocyte hyperplasia and enhanced agonist-induced platelet activation in vasodilator-stimulated phosphoprotein knockout mice. *Proc Natl Acad Sci U S A*. 1999;96:8120-8125.
 74. Aszodi A, Pfeifer A, Ahmad M, et al. The vasodilator-stimulated phosphoprotein (VASP) is involved in cGMP- and cAMP-mediated inhibition of agonist-induced platelet aggregation, but is dispensable for smooth muscle function. *EMBO J*. 1999;18:37-48.
 75. Massberg S, Gruner S, Konrad I, et al. Enhanced in vivo platelet adhesion in vasodilator-stimulated phosphoprotein (VASP)-deficient mice. *Blood*. 2004;103:136-142.
 76. Suzuki T, Nakashima S, Nozawa Y. Inhibition of phosphatidylinositol 4-phosphate 5 kinase by cyclic AMP in human platelets. *Platelets*. 1994;5: 258-265.
 77. Heemskerk JMW, Sage SO. Calcium signalling in platelets and other cells. *Platelets*. 1994;5:295-316.
 78. de Chaffoy de Courcelles D, Roevens P, van Belle H. Agents that elevate platelet cAMP stimulate the formation of phosphatidylinositol 4-phosphate in intact human platelets. *FEBS Lett*. 1986;195:115-118.
 79. Rynningen A, Jensen BO, Holmsen H. Elevation of cyclic AMP decreases phosphoinositide turnover and inhibits thrombin-induced secretion in human platelets. *Biochim Biophys Acta*. 1998;1394:235-248.
 80. Manns J, M., Brennan KJ, Colman RW, Sheth SB. Differential regulation of human platelet responses by cGMP inhibited and stimulated cAMP phosphodiesterases. *Thromb Haemost*. 2002;87: 873-879.